

Modal mineralogy, textural data and geochemical data for caldera-facies Hells Mesa Tuff and a comagmatic lava dome, with selected data plots and supporting map data

New Mexico Bureau of Geology and Mineral Resources Open-file report 458

by

Richard M. Chamberlin

NOTE: This report has been superceded by OFR-568
<https://geoinfo.nmt.edu/publications/openfile/details.cfm?Volume=568>

December, 2001

CONTENTS:

Introduction.....4
 Methods.....6
 Geologic Map Data.....8
 Modal Mineralogy and Textural Data.....12
 Whole-rock Geochemical Data.....13
 References.....17

TABLES:

1. Modal mineralogy and textural data for caldera-facies Hells Mesa Tuff and a comagmatic lava dome.....18
 2. Whole-rock geochemical data for caldera-facies Hells Mesa Tuff and a comagmatic lava dome.....19
 3. Modal mineralogy (volume %) and maximum crystal size (mm) from a measured section of the Hells Mesa Tuff outflow sheet near Magdalena (Brown, 1972).....20
 4. Modal mineralogy (volume %) and maximum crystal size (mm) for the Hells Mesa eruptive sequence.....21
 5. Whole-rock geochemical data available for the Hells Mesa magmatic suite (n =51).....22
 6. Whole-rock geochemical data for unaltered and slightly altered samples of the Hells Mesa magmatic suite (n=11).....23
 7. Whole-rock geochemical data for post-Hells Mesa rhyolites in the eastern Socorro caldera.....24

FIGURES:

1. Structural index map of the eastern Socorro caldera.....25
 2. Geologic map of the Bursum mine area.....26
 3. Geologic map of the Torreon Springs area.....27

4.	Geologic map of the Esperanza mine area.....	28
5.	Schematic stratigraphic section of Hells Mesa facies in the eastern Socorro caldera.....	29
6.	Quartz content vs relative stratigraphic position for the Hells Mesa eruptive sequence.....	30
7.	Maximum crystal size vs crystallinity for the Hells Mesa eruptive sequence.....	31
8.	Ba vs. sanidine content for unaltered Hells Mesa rocks at the Esperanza Mine and a sanidine-granite clast in dome-derived tuff breccias.....	32
9.	SiO ₂ vs. groundmass (melt) content in caldera-facies Hells Mesa rocks.....	33
10.	K ₂ O/Na ₂ O vs Na ₂ O for K-metasomatized Hells Mesa rocks near the Bursum mine and unaltered Hells Mesa rocks near the Esperanza mine.....	34
11.	Histogram showing SiO ₂ variation in the Hells Mesa eruptive suite (n = 34). Normalized data from Table 5.....	35
12.	Nb vs. Zr/TiO ₂ for Oligocene rhyolites erupted from the eastern Socorro caldera at 31.9, 30.0, 28.8 and 28.7 Ma. Data from Tables 2 and 7.....	36
13.	Total alkali--silica classification of unaltered Hells Mesa magmatic suite (Cox, 1979). Data from Table 6.....	37
14.	Immobile element discrimination diagram (SiO ₂ vs. Zr/TiO ₂) for unaltered Hells Mesa magmatic suite (Wincheseter and Floyd, 1977). Data from Table 6.....	38
15.	Immobile element discrimination diagram (Zr/TiO ₂ vs. Nb/Y) for unaltered Hells Mesa magmatic suite (Winchester and Floyd, 1977). Data from Table 6.....	39

INTRODUCTION

This report presents phenocrystic mineral modes, textural data and geochemical data for caldera-facies Hells Mesa Tuff, a slightly younger comagmatic lava dome, and dome-derived tuff breccias that are exposed in the eastern and southwestern sectors of the Socorro caldera (Fig1). This data is presented in support of an article entitled *Waning-stage Eruptions of the Oligocene Socorro Caldera, Central New Mexico*, which has been submitted for publication by the New Mexico Natural History Museum in their Bulletin 18, *Volcanology in New Mexico* (Chamberlin, in press). This new data set supplements detailed geologic mapping of the Luis Lopez quadrangle (Chamberlin and Eggleston, 1996) and a recent $^{40}\text{Ar}/^{39}\text{Ar}$ geochronology study of the eastern sector of the Socorro caldera (Chamberlin, McIntosh and Eggleston, in press).

Additional Note: Recent mapping (12/01), has shown approximately 30m of upper Hells Mesa lag breccias are present north of the Esperanza mine (thus, Fig.5 of this report supersedes fig. 2 of Chamberlin, 2001). These revised map relationships are shown on Figure 4, and described on p. 11.

Three new data sets are presented: 1) detailed geologic maps of upper caldera-facies Hells Mesa Tuff and a comagmatic lava dome with derivative tuffs, showing maximum-clast-size distribution patterns of comagmatic-lithic lag breccias, inferred vent areas, and locations of 14 representative samples (Figs. 2-4); 2) modal mineralogical and textural analyses of 14 representative thin sections by the author using a Ziess petrographic microscope and Swift automatic point counter (Table 1); and 3) X-ray fluorescence spectrometry analyses of 9 (of 14) whole-rock samples done by Chris McKee at the NMBG/NMT XRF lab to determine major oxide concentrations and abundance of 17 trace elements (Table2). These new data sets allow

comparison of modal mineralogy with geochemical trends in the upper caldera facies tuffs and the comagmatic lava dome. Three of the 14 samples were collected from the xenolith-poor top of the underlying lower caldera-facies Hell Mesa Tuff; again to allow comparison. Thin sectioned samples from the Torreon Springs area have not been chemically analysed.

New data are compared to and integrated with published and unpublished data sets from previous investigations that represent: 1) the densely welded Hell Mesa outflow sheet near Magdalena (modal mineralogy; Brown, 1972); 2) hydrothermally altered and mineralized caldera-facies lower Hells Mesa Tuff (whole-rock geochemistry; Eggleston et al., 1983); and 3) random samples of K-metasomatized Hells Mesa Tuff and recycled Hells Mesa clasts in younger metasomatized formations collected to study the chemistry and mineralogy of K-metasomatism in the Socorro region (whole-rock geochemistry; Ennis, 1996).

C.E. Chapin graciously provided archived thin sections from Brown's measured section of the outflow sheet (Brown, 1972) so the author could make measurements of maximum crystal sizes in the densely welded tuffs. Maximum-crystal-size data, Brown's original modal data, and the stratigraphic position of samples are all listed in Table 3. Data from Table 3 are combined with modal data from this study (Table 4) in order to examine mineralogical trends for the entire Hells Mesa sequence with respect to their relative stratigraphic position. Available and complete whole-rock geochemical analyses (i.e. include LOI data) for the Hells Mesa eruptive suite are listed in Table 5 (n=51). Seventeen of these available analyses apparently represent moderately to intensely altered rocks, mineralized rocks and inaccurate analyses; the latter are indicated by statistical outlier values or high totals. The remaining 34 analyses, which include 23 K-metasomatized samples, are used to calculate mean SiO₂ content of the Hells Mesa eruptive suite, since the SiO₂ content of tuffs is not significantly affected by K-metasomatism (Dunbar et.

al., 1994). Analyses of 11 unaltered to slightly altered Hells Mesa rocks are listed in table 6; mean values of these samples are considered to be the most representative of the Hells Mesa magmatic suite (not considering volatiles elements). Finally, new geochemical data for the upper Hells Mesa tuffs and comagmatic lava dome are compared to geochemical data from post Hells Mesa rhyolite units erupted from the eastern Socorro caldera (Table 7; Chamberlin et. al., in press); this allows an examination of upper-crustal magmatic evolution over a span of 3.2 million years (31.9-28.7 Ma).

Data plots were made from the above data sets using *Minpet for Windows*. This software package also was used to calculate basic statistics and correlation coefficients. Geochemical rock classification diagrams of the relatively unaltered Hells Mesa magma suite, without K-metasomatized samples (Table 6, n=11), were also made using the Minpet software from data normalized to total 100% on a nonvolatile basis.

METHODS

Geologic mapping of the upper-caldera facies Hells Mesa Tuff, and tuff breccias derived from a comagmatic lava dome (Figs. 1-4), emphasized field measurements of the maximum size of comagmatic clasts within outcrops of the crudely bedded coignimbrite lag breccias. Mapping traverses were made primarily along strike to observe lateral variations in one or more depositional units units at about the same stratigraphic level. Secondary traverses were made roughly perpendicular to strike at spacings of about 100-200 m, as outcrop patterns permitted or dictated. Clast sizes were measured with a 33 cm-long rock hammer graduated at 5cm and 1cm increments. Field measurements of larger clasts (>50 cm) are considered to be accurate to ± 5 cm and smaller clasts to $\pm 1-2$ cm.

Petrographic analyses of thin sections (Table 2) were completed using a Zeiss petrographic microscope. Maximum phenocryst sizes were measured with the petrographic microscope using a graduated eyepiece (one division = 0.038 mm at a magnification of 31.25x). Thin sections were scanned with a hand lens to locate the largest crystal, which was then measured to the nearest 0.1 mm (± 0.1 mm). Modal mineral analyses were made using a Swift automatic point counter set at an interval spacing of 1mm by 1mm, which is approximately equal to the mean phenocryst size for most of these crystal-rich rocks. Mineral species were identified using optical properties as catalogued by Kerr (1959) and by Deer, Howie and Zussman (1966). In unaltered rocks, untwinned sanidine crystals could only be confidently discriminated from quartz by obtaining interference figures (as point counts progressed). In K-metasomatized samples from the Bursum mine area, plagioclase phenocrysts are completely replaced by delicate lattice-works of adularia and clay minerals that commonly wash out out the thin section during preparation. Euhedral holes with bits of clay along the edges are counted as phenocrystic plagioclase in these altered rocks; likewise rhombic outlines associated with leucoxene are counted as sphene crystals.

Three repeated analyses of one sample (Table 2, E1) indicate that counting errors decrease with increasing abundance of a mineral phase. Total phenocryst contents are estimated to be reproducible to about ± 2 vol. % at a total of 40 vol. % crystals. Counting errors for phenocrystic quartz are estimated at $\pm 10\%$ at a total quartz content of 10%. Errors for minor phases such as biotite and magnetite/hematite are as high as $\pm 50\%$. Coarse grained samples (phenocrysts > 5 mm) yield more erratic volumetric estimates of modal mineralogy because of the "nugget" effect, which is exacerbated by a small sample size (standard thin section $\sim 22 \times 40$

mm). Total crystal contents for coarse grained rocks are probably reproducible at about ± 5 vol. %.

Four samples from the Bursum mine area and five samples from the Esperanza mine area were submitted for whole-rock geochemical analyses at the NMBG XRF lab. Analytical methods are described in the footnote to Table 2. Repeat analyses at the NMBG XRF lab (n=148) indicate wt% SiO₂ concentrations are reproducible to ± 1.1 wt. % at a total silica content of 71.35 wt % (95% confidence, $\pm 2\sigma$). Other oxide concentrations are precise to about ± 2 -3%, except for P₂O₅ ($\pm 10\%$). Trace element analyses are reproducible to ± 10 -25 %, except for As, V, Mo and Cr, which have associated analytical errors of ± 35 -70% (as the method approaches detection limits for these elements).

GEOLOGIC MAP DATA

Crystal-rich, caldera-facies Hells Mesa Tuff is divided into lower and upper members on the basis of the lithology of entrained lithic fragments (Chamberlin and Eggleston, 1996; Fig 1). The lower caldera-facies Hells Mesa contains a variety of older Tertiary volcanic fragments (mostly andesites) and clasts of pre-Tertiary rocks such as limestone, sandstone, schist and granitic rocks. Fragments of older country rock that occur in the densely welded tuffs are referred to as *xenoliths*. The basal caldera-facies tuffs are xenolith rich and contain large blocks of older country rock interpreted as landslide megabreccias derived from contemporaneous collapse of an oversteepened caldera wall (along the south margin). The top of the lower caldera-facies Hells Mesa Tuff is xenolith-poor. In general, the lower caldera-facies Hells Mesa Tuff can be referred to as xenolithic, or xenolith bearing. Near Torreon Springs the top 20m of the lower xenolithic member is moderately to poorly welded and forms a recessive valley or swale between the lower and upper members. Stratigraphic relationships of caldera-facies Hells Mesa Tuff (in the eastern

sector of the caldera) and a slightly younger ring-fracture lava dome and derivative tuff breccias are schematically illustrated in Figure 5. Local facies of the upper Hells Mesa Tuff near Torreon Springs occupy the same stratigraphic position as the bedded tuff zone (Thuf) at the Bursum mine.

The upper caldera-facies Hells Mesa Tuff tends to be crudely bedded and contains abundant to rare fragments of red crystal-rich rhyolite compositionally similar or identical to the enclosing crystal-rich tuffs. These red rhyolite clasts are referred to here as comagmatic lithics (synonymous with autoliths). Field relationships and textural characteristics support their interpretation as coignimbrite lithic lag breccias (clasts of normal density) carried only a few kilometers from their source vent (Wright and Walker, 1977).

Near the Bursum mine, the depositional contact between the lower and upper members of the caldera-facies Hells Mesa Tuff is gradational and densely welded. This subtle contact is marked by the upward disappearance of rare small andesitic xenoliths and appearance of rare small clasts of red spherulitic rhyolite near the base of a 200m thick massive zone. A thin fine-grained ash-fall bed occurs about 10 meters above this subtle gradational contact between lower and upper Hells Mesa Tuff. A poorly welded recessive zone about 20m thick locally occurs at the top of the massive lower zone. Above this cooling break, a distinctly bedded zone (~ 200m thick) contains numerous fall deposits and coarse comagmatic lag breccias. About 15-20 ledge-forming depositional units are visible on aerial photographs of the upper bedded zone, where well exposed about 1 km ESE of the Bursum mine.

A 2-cm-thick "sandy" winnowed layer (~ 90% fine- to medium-grained crystals) occurs immediately above an ash-rich fall deposit near the base of the bedded zone (outcrop location shown on Fig.2). This rare lithology extends a few tens of meters along strike. It may represent

a "volatiles-jet" separation of heavier crystals from finer-grained ash at the toe of an advancing pyroclastic flow or some other type of high-velocity wind deposit.

Detailed geologic maps of the the Bursum mine, Torreon Springs and Esperanza mine areas are shown as Figs. 2-4. Mapping concentrated on determining maximum clast size distribution patterns in the crudely bedded ignimbrites and comagmatic lag breccias. Field observations of clast textures and clast geometries (commonly angular to equant) indicate that most of them were emplaced at normal rock densities and do not represent compacted pumice. However, some moderately flattened spherulitic clasts in the Bursum mine area apparently represent "soft" slightly compressible microcrystalline mush at the time of emplacement. The maximum clast size observed in an average continuous outcrop (eg. ~10 -20 m long) is commonly about twice the size of the most abundant megascopic clasts. Distribution patterns of maximum clast size are used to estimate the general transport direction of the lag breccia deposits and the approximate distance from the coarsest outcrops to the inferred vent area (Figs. 1-4).

The "downstream" distance, through which the maximum clast size decreases by a factor of two, can be used as a rough indicator of the average transport energy associated with a particular vent area. This "transport-energy factor" is about 1300-1400 m for the lag breccias near Torreon Springs, about 500-600 m for the Bursum mine facies and 400-500 m for the Esperanza mine facies. Post-depositional rift faulting has clearly distorted (stretched) the maximum-clast-size isopleths near the Bursum mine (Fig. 2). Vent areas are inferred where extrapolated clast sizes approach 3-6 m in the "upstream" direction.

Lag breccias near the Bursum mine are characterized by clasts of phenocryst-rich rhyolite that exhibit spherulitic crystallization of the red groundmass. Lag breccias in the Torreon

Springs area are formed by angular fragments of densely welded lower Hells Mesa Tuff that occasionally contain smaller xenoliths of dark gray andesite within the younger generation of explosively fragmented (recycled) ignimbrite. Blocky tuff breccias near the Esperanza mine (Trt) are lithologically equivalent to the crest of the small lava dome exposed about 1 km to the south; these northward fining breccias were apparently erupted from a vent near the north flank of the dome (Fig. 4).

The comagmatic lag breccias are crudely zoned within the local facies of bedded ignimbrites that are derived from different vent areas. The Bursum mine facies coarsens upwards through as much as 400 m of mostly densely welded tuffs. Breccia clasts as much as 75 cm long occur near the top of the Bursum mine sequence. The Torreon Springs facies appears to be coarsest near the middle of the 200m thick unit. Complete sections of moderately welded tuffs, which are exposed in fault blocks west of Torreon Springs (Fig.3), coarsen upwards toward the medial zone and then fine upwards toward the top of the map unit. The lower, medial and upper breccia zones near Torreon Springs generally become finer grained to the south-southwest, although the pattern is more erratic than at the Bursum mine or the Esperanza mine. The poorly to moderately welded dome-derived tuffs north of the Esperanza mine are coarsest near the base of the 60-120m thick sequence. This basal blocky breccia unit coarsens uniformly toward the south and the exposed crest of the coeval lava dome (Fig. 4).

Approximately 30 m of mostly densely welded "Thu" equivalent conformably underlie the blocky tuff breccias (Trt) north of the Esperanza mine. Red rhyolitic clasts in this thin zone are small (2-10cm) and sparse (1-3%). Small andesitic lithics also occur rarely, which locally makes this thin zone difficult to distinguish from the underlying xenolith-poor, lower Hells Mesa Tuff (Thx). About 0.7 km north of the Esperanza mine, the uppermost 7m of Thu is a friable

poorly welded zone; this welding break suggests a moderate hiatus of $\sim 10^3$ - 10^4 years between upper Hells Mesa pyroclastic eruptions and emplacement of the coarserly porphyritic lava dome.

Inferred vent areas for the upper lag-breccia facies and the comagmatic lava dome roughly define an inner ring fracture zone about 7 km in diameter (Fig.1). The elliptical shape shown on Fig. 1 reflects post-caldera stretching (crustal extension) to the WSW, which is associated with the Rio Grande rift.

MODAL MINERALOGY AND TEXTURAL DATA

Modal mineralogy and textural data for 14 thin sections of caldera-facies Hells Mesa Tuff and a comagmatic lava dome with associated tuffs are summarized in Table 1. The Hells Mesa Tuff exhibits a phenocrystic mineral suite characteristic of a metaluminous arc-related rhyolite. In order of decreasing overall abundance, the major mineral phases are sanidine, plagioclase and quartz with minor biotite and opaques (magnetite/hematite). Trace amounts of sphene, apatite and zircon are typical of most samples from the Hells Mesa. A few reflected light observations and mass-balance comparison of geochemical data (i.e. TiO_2 and $\text{TiO}_2/\text{Fe}_2\text{O}_3$) with modal mineralogy (Tables 1 and 2) suggest that ilmenite is not present as a significant component of the opaques.

Samples were collected in order to represent each major lithology observed in the upper caldera-facies tuffs and the dome-derived tuff breccias. These lithologies include: crystal-rich tuff, crystal-rich comagmatic breccia clasts, and the lava dome itself. Rare clasts of granite observed in the Torreón Springs and Esperanza mine facies tuffs were also collected to evaluate their origin.

Samples E1 and E2 both represent the comagmatic lava dome, although the latter is from a 3.1m block of flow-banded rhyolite within the dome derived tuffs (Fig.4). Field relationships, identical mineral suites, and equivalent textures (such as compositionally zoned sanidine crystals) all indicate these samples are from the same eruptive unit. However, the dome sample contains significantly less crystals (45%) versus the lava block, which contains ~59 % crystals. The average of these two analyses, 52 vol. %, is considered to be the best estimate for the total crystal content of the lava dome. The large variation in measured crystal content is attributed to nonuniform melt distribution in the granular mush (possibly related to dilation along shears; eg. Smith, 1997) and the "nugget" effect of coarse phenocrysts of sanidine and quartz that occur in the relatively small samples (standard thin sections, 22 x 40 mm).

Upper Hells Mesa Tuffs and the slightly younger comagmatic lava dome are all quartz rich and crystal rich. A plot of quartz content versus relative stratigraphic position shows that the top of outflow facies at Magdalena is approximately correlative to the top of the lower caldera-facies Hells Mesa Tuff (Fig 6). The maximum size of phenocrysts in the Hells Mesa outflow and caldera-facies units shows a positive correlation with crystallinity, or total phenocryst content (Fig. 7).

Granite clasts near the Esperanza mine are mineralogically very similar to the Hells Mesa Tuff (Table 1; E4 & E5). However, these sanidine granites lack compositionally zoned sanidine phenocrysts typical of the Hells Mesa-age lava dome (31.89 ± 0.16 Ma; Chamberlin et al., in press) and the dome-derived tuffs (Table 1). Chemical data, see following section, indicate the sanidine-granite clasts are not comagmatic with the Hells Mesa Tuff, even though they are mineralogically similar. Rare granite clasts near Torreon Springs (Table 1, T3; Fig. 3) contain

abundant microcline and traces of monazite; they are clearly derived from Proterozoic basement rocks.

WHOLE-ROCK GEOCHEMICAL DATA

Whole-rock geochemical data for 9 samples collected from caldera-facies Hells Mesa-age rocks are listed in Table 2. Two of these samples are from the xenolith-bearing lower Hells Mesa Tuff and seven are from the stratigraphically higher upper Hells Mesa and the stratigraphically youngest lava-dome related rocks (Fig. 5). One sample of sanidine granite was analysed; it was collected from the basal blocky zone of the dome-derived tuffs north of the Esperanza mine (Fig 4, E4).

A plot of Ba content vs. sanidine content (Fig.8) demonstrates a strong correlation ($r^2 = 0.99$) for different stratigraphic levels of Hells Mesa rocks; and that the sanidine-granite clast is not comagmatic with the Hells Mesa rocks. This unusual lithology (i.e. high-temperature alkali feldspar in a coarse-grained "low temperature" plutonic rock) is interpreted as a partially melted --contact metamorphosed-- pendants of Proterozoic granite that were stoped from the walls of the Hells Mesa magma chamber prior to eruption of the dome-related tuffs. Mylonitic shear bands and cataclastic textures in clasts of sanidine granite from the same locality suggest high temperature shearing and possibly explosive deformation of the pendants during eruption of the dome-derived tuffs. Sanidine-granite clasts are about twice the size of adjacent lava blocks in the tuff breccia outcrop ~1 km north of the lava dome (Fig.4). This size difference suggests that these unusual sanidine-granite clasts were carried rapidly upward from considerable depth by the pyroclastic eruption column and followed a different (higher) trajectory during emplacement. Rapid transport of these partially melted pendants of granite from the magmatic temperature environment to the surface caused quenching and preservation of the high-temperature sanidines.

Petrographic data and field relationships indicate that samples E1 and E2 are from the same lava dome, although the latter is from a large block in the dome-derived tuff breccia. At first glance, geochemical data, particularly SiO_2 content (Table 2), suggest that they are not genetically equivalent rocks. Slightly higher Fe_2O_3 , TiO_2 , V, Y, and Zr contents in E2 are readily explained by a higher content of opaques and slightly more sphene (Table 1). Sample E2 also contains minor calcite (~2%, note relatively high CaO content), which partially replaces plagioclase. Thus the SiO_2 content in this sample is slightly depressed (~ 1%) by the presence of secondary calcite. The ~ 5% difference in normalized SiO_2 content ($n\text{SiO}_2$, Table 2) is almost certainly real; this relationship suggests that the groundmass of the lava is a high-silica rhyolite (~77.5 % SiO_2) and that the feldspar-rich sample (E2) essentially forms a diluted melt (feldspars average about 65% SiO_2 , Deer, Howie and Zussman, 1966). Normalized SiO_2 shows a moderate positive correlation with total melt content ($r^2 = 0.69$) for the waning-stage Hells Mesa rocks and the uppermost lower Hells Mesa Tuff (Fig. 9), which supports the above suggestion.

Samples from the Bursum mine area (B1-B4) are potassium metasomatized. K-metasomatism is best verified in thin section, but it is also typically indicated by $\text{K}_2\text{O}/\text{Na}_2\text{O}$ ratios above 4 and commonly by Na_2O concentrations less than 2.0 wt % (Fig. 10). Soda, potash, Rb, Sr, Ba and other mobile elements have been redistributed by metasomatism in the Bursum mine area and are not representative of compositional trends in the Hells Mesa magma chamber.

Thirty four analyses of relatively unaltered and K-metasomatized rock samples from the Hells Mesa eruptive suite (Table 5, select) yield a mean normalized silica content of 73.4 ± 1.5 wt. % SiO_2 . A histogram of silica content for the Hells Mesa suite shows that most samples range from 69-75 % SiO_2 (Fig. 11). The silica content of a welded tuff is generally unaffected by K-metasomatism (Dunbar, et.al., 1994).

The magmatic evolution of 4 rhyolitic eruptive centers in the eastern Socorro caldera, from 31.9 to 28.7 Ma, is illustrated by a plot of Zr/TiO₂ vs Nb as shown in Fig. 12. From youngest to oldest the eruptive units are: La Jencia Tuff, upper rhyolite member of Luis Lopez Formation, medial tuff Member of Luis Lopez Formation, and Hells Mesa Tuff: dated respectively at 28.7, 28.8, 30.0 and 31.9 Ma (Fig. 12; Chamberlin et. al., in press). The diagram illustrates a general decrease in Nb content with time for the older two units, and a later increase in Zr/TiO₂ ratio with time. The origin of these magmatic trends is beyond the scope of this data presentation.

Unaltered samples of the Hells Mesa magmatic suite (Table 6) are plotted on a total alkali--silica classification diagram (Fig. 13). Their classification as rhyolites is consistent with the observation of abundant phenocrystic quartz and sanidine in hand specimens (Chamberlin and Eggleston, 1996). It is inappropriate to plot K-metasomatized and hydrothermally altered samples on a total alkali--silica diagram.

Immobile element discrimination diagrams have been used in to classify the magmatic series of hydrothermally altered samples (Winchester and Floyd, 1977). Immobile element plots for unaltered rocks of the Hells Mesa suite (Table 6) are shown as Figs. 14 and 15. The plot of SiO₂ vs Zr/TiO₂ (Fig. 14) classifies the Hells Mesa suite as transitional between rhyolites and dacites. The Zr/TiO₂ vs Nb/Y plot (Fig. 15) indicates a "trachyandesite" composition for these silica-rich rocks. Zr/TiO₂ is a proxy for silica content and Nb/Y is proxy for alkalinity (i.e., total alkalis). The relatively low Zr content and slightly elevated Y content of the Hells Mesa magma suite has "pushed" it into the trachyandesite domain; perhaps this reflects a "parental" andesitic arc-related magma that evolved into the rhyolitic Hells Mesa suite.

REFERENCES:

- Brown, D. M., 1972, Geology of the southern Bear Mountains, Socorro County, New Mexico: M.S. Thesis, New Mexico Institute of Mining and Technology, 110 p. New Mexico Bureau of Mines and Mineral Resources, Open-file Report 42, 110 p.
- Chamberlin, R.M., 2001, Waning-stage Eruptions of the Oligocene Socorro Caldera, Central New Mexico, *in* Volcanology in New Mexico, L.S. Crumpler and S.G. Lucas (eds.), New Mexico Museum of Natural History and Science Bulletin 18, p. 69-77.
- Chamberlin, R. M. and Eggleston, T. L., 1996, Geologic map of the Luis Lopez 7.5 minute quadrangle, Socorro County, New Mexico: New Mexico Bureau of Mines and Mineral Resources Open-file Report 421, 147 p.
- Chamberlin, R.M., McIntosh, W.C. and Eggleston, T L., in press, $^{40}\text{Ar}/^{39}\text{Ar}$ Geochronology and Eruptive History of the Eastern Sector of the Oligocene Socorro Caldera, Central Rio Grande Rift, New Mexico: *in* Tectonics, Geochronology and Volcanism in the Southern Rocky Mountains and Rio Grande Rift; S.M. Cather, W. C. McIntosh, and S.A. Kelly (eds.): New Mexico Bureau of Geology and Mineral Resources Bulletin 160
- Cox, K.G., Bell, J.D., and Pankhurst, R.J., 1979, *The interpretation of Igneous Rocks*: London: Allen and Unwin, 450 p.
- Deer, W. A., Howie, R. A., and Zussman, J., 1966, An introduction to the rock-forming minerals: Wiley and Sons, New York, N. Y., 528 p.
- Dunbar, N.W., Chapin, C.E., Ennis, D.J. and Campbell, A.R., 1994, Trace element and mineralogical alteration associated with moderate and advanced degrees of K-metasomatism in a rift basin at Socorro, New Mexico: New Mexico Geological Society Guidebook 45, p. 225-231.
- Eggleston, T.L., Norman, D.I., Chapin, C.E. and Savin, S., 1983. Geology, Alteration and genesis of the Luis Lopez manganese district, New Mexico: New Mexico Geological Society Guidebook 34, p. 241-246.
- Ennis, D.J., 1996, The effects of K-metasomatism on the mineralogy and geochemistry of silicic ignimbrites near Socorro, New Mexico: M.S.thesis, New Mexico Institute of Mining and Technology, Socorro, New Mexico, 160 p.
- Kerr, P. F., 1959, Optical Mineralogy, McGraw Hill, New York, 442 p.
- Norrish, K. and Chappell, B. W., 1977, An accurate X-ray fluorescence spectrographic method for the analysis of a wide range of geologic samples: *Geochimica Cosmochimica Acta*, v. 33, p. 67-76.
- Norris, K. and Hutton, J. T., 1969, X-ray fluorescence spectrometry, *in Physical Methods in Determinative Mineralogy*, ed. Zussman, Academic Press.
- Spradlin, E. J., 1972, Stratigraphy of Tertiary Volcanic Rocks, Joyita Hills Area, Socorro County, New Mexico: unpub. M. S. Thesis, University of New Mexico, 73p.
- Winchester, J.A. and Floyd, P.A., 1977, Geochemical discrimination of different magma series and their differentiation products using immobile elements: *Chemical Geology*, v.20, p.325-343.
- Wright, J.V., and Walker, G.P.L., 1977, The ignimbrite source problem, significance of a co-ignimbrite lag-fall deposit: *Geology*, v. 5, p. 729-732.

Detailed Figure Captions:

Figure 1. Structural index map of the eastern Socorro caldera. Generalized from Chamberlin et al., in press; Osburn et al., 1986, and this report (Figs. 2–4). CHB is a magmatically uplifted central horst block.

Figure 2. Geologic map of the Bursum mine area. Modified after Chamberlin and Eggleston, 1996. White areas are post-Luis Lopez age strata, mostly Santa Fe Group basin-fill deposits.

Figure 3. Geologic map of the Torreon Springs area. Modified after Osburn et al., 1986.

Figure 4. Geologic map of the Esperanza mine area. Modified after Chamberlin and Eggleston, 1996.

Figure 5. Schematic stratigraphic section of the Hells Mesa facies in the eastern Socorro caldera. Modified after Chamberlin et al. (in press). Contacts are dashed where gradational, solid at cooling breaks, and queried where not exposed. The Torreon Springs facies of the upper Hells Mesa Tuff occupies the same stratigraphic position as the upper bedded zone east of the Bursum mine (Thuf). Note, this figure supersedes a similar figure shown as fig. 2 in Chamberlin, 2001.

Figure 6. Quartz content vs. relative stratigraphic position for the Hells Mesa eruptive sequence. Data from Brown (1972) and Table 1. Symbol size reflects a counting error of $\pm 10\%$.

Figure 7. Maximum crystal size vs. crystallinity for the Hells Mesa eruptive sequence. Data from Tables 1 and 3. Crystallinity-flow barrier from Marsh (1981). Symbol size reflects $\pm 2\%$ counting error for medium-grained samples and $\pm 5\%$ counting error for coarse-grained samples.

Figure 8. Ba vs. sanidine content for unaltered Hells Mesa rocks near the Esperanza mine and a sanidine-granite clast in dome-derived tuff breccia. Data and sample numbers from Tables 1 and 2.

Figure 9. SiO_2 vs. groundmass (melt) content in caldera-facies Hells Mesa rocks. Data and sample numbers from Tables 1 and 2.

Figure 10. $\text{K}_2\text{O}/\text{Na}_2\text{O}$ vs. Na_2O for K-metasomatized Hells Mesa rocks near the Bursum mine and unaltered Hells Mesa rocks near the Esperanza mine. Data and sample numbers from Table 2.

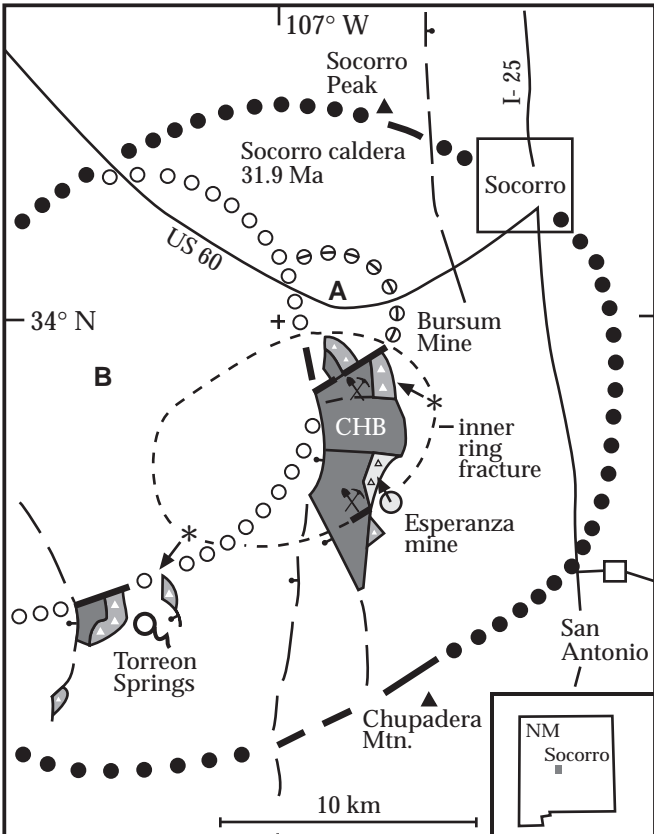
Figure 11. Histogram showing SiO_2 variation in the Hells Mesa eruptive suite ($n = 34$). Normalized data from Table 5.

Figure 12. Nb vs Zr/TiO_2 for Oligocene rhyolites erupted from the eastern Socorro caldera. Data from Tables 2 and 7.

Figure 13. Total alkali-silica classification of unaltered Hells Mesa rocks (Cox, 1979). Data from Table 6.

Figure 14. Immobile element discrimination diagram (SiO_2 vs. Zr/TiO_2 for unaltered Hells Mesa rocks (Winchester and Floyd, 1977). Data from Table 6.

Figure 15. Immobile element discrimination diagram (Zr/TiO_2 vs. Nb/Y) for unaltered Hells Mesa rocks (Winchester and Floyd, 1977). Data from Table 6.



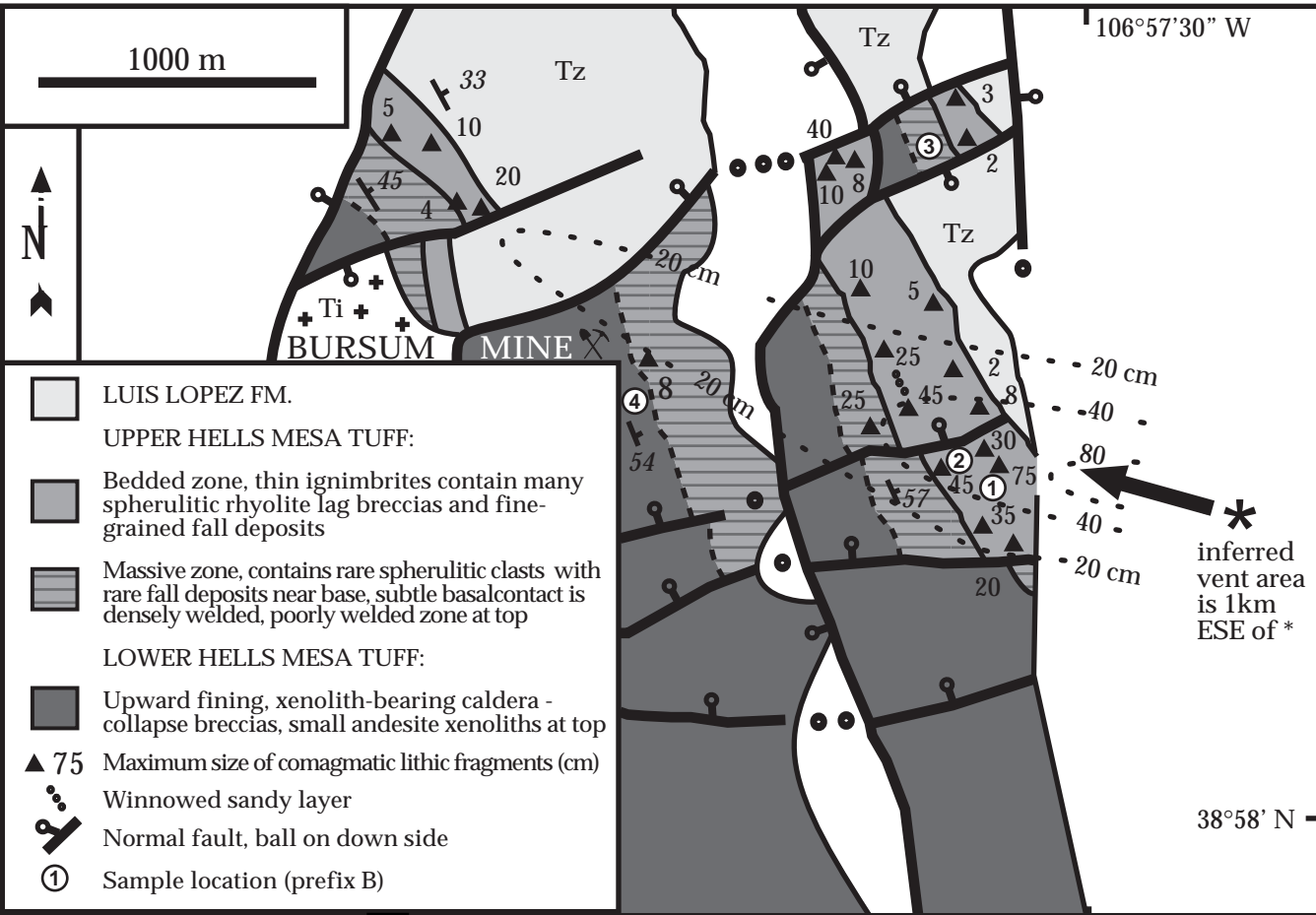
- — Outer ring fracture zone of Socorro caldera, dashed where approximately located, dotted where concealed
 - Hells-Mesa-age lava dome (vent area)
 - △△△ dome-derived tuffs
 - ▲▲▲ upper caldera-facies Hells Mesa Tuff, contains comagmatic lag breccias
 - lower caldera-facies Hells Mesa Tuff, contains abundant to sparse xenoliths
 - ↖* inferred vent area for upper Hells Mesa Tuff and transport direction of lag breccias
 - ↘ rift fault, ball on down side
 - ⌘ manganese mine (abandoned)
- YOUNGER ERUPTIVE CENTERS:
- ⊖⊖⊖ **A** Black Canyon vent area, 30.0 Ma
 - **B** Sawmill Canyon caldera, 28.7 Ma











1000 m



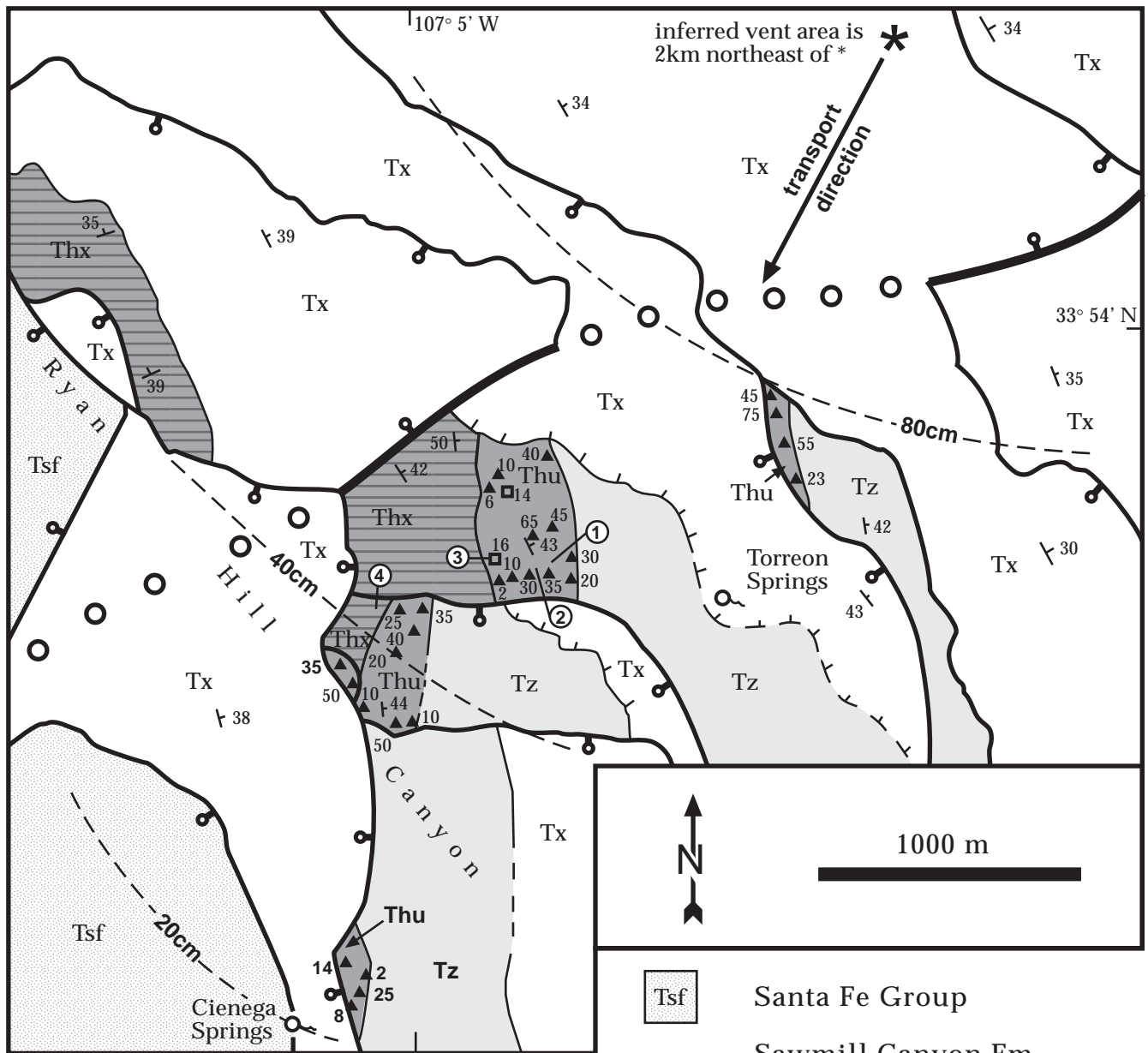
106°57'30" W



-  LUIS LOPEZ FM.
- UPPER HELLS MESA TUFF:
 -  Bedded zone, thin ignimbrites contain many spherulitic rhyolite lag breccias and fine-grained fall deposits
 -  Massive zone, contains rare spherulitic clasts with rare fall deposits near base, subtle basalcontact is densely welded, poorly welded zone at top
- LOWER HELLS MESA TUFF:
 -  Upward fining, xenolith-bearing caldera-collapse breccias, small andesite xenoliths at top
-  75 Maximum size of comagmatic lithic fragments (cm)
-  Winnowed sandy layer
-  Normal fault, ball on down side
-  1 Sample location (prefix B)

*
inferred vent area
is 1km
ESE of *

38°58' N



ring fracture zone of Sawmill Canyon caldera



southern topographic wall of Sawmill Canyon caldera



normal fault, ball on downthrown block



maximum size of "comagmatic" lithic fragment (cm)



maximum size of rare microcline-granite xenolith



sample location (prefix T)



Tsf Santa Fe Group



Tx Sawmill Canyon Fm., La Jenica Tuff, and younger tuffs



Tz Luis Lopez Formation



Thu upper Hells Mesa Tuff, contains abundant to sparse lithic fragments of "recycled" xenolith-poor lower Hells Mesa Tuff



Thx lower Hells Mesa Tuff, contains abundant to sparse andesitic xenoliths, partially welded zone at top

Tz

LUIS LOPEZ FM.



Dome-derived tuffs with angular lava blocks and clasts



Hells Mesa Tuff-age lava dome



upper Hells Mesa Tuff with spherulitic comagmatic lithic fragments



xenolith-bearing lower Hells Mesa Tuff



90 maximum size of comagmatic lithic fragments (cm)



100 maximum size of rare sanidine - granite xenoliths (cm)



① sample location (prefix E)



basal non-welded avalanche deposit with well-rounded lava clasts



Normal fault



Reverse fault

HORST BLOCK

1000 m

106°57'30" W

ESPERANZA MINE

VENT

INNER RING FRACTURE

CREST OF LAVA DOME

38° 58' N

Tz

④

②

①

⑤

⑧

⑩

③

⑥

⑦

⑨

⑪

⑫

⑬

⑭

⑮

⑯

⑰

⑱

⑲

⑳

㉑

㉒

㉓

㉔

㉕

㉖

㉗

㉘

㉙

㉚

㉛

㉜

㉝

㉞

㉟

㊱

㊲

㊳

㊴

㊵

㊶

㊷

㊸

㊹

㊺

㊻

㊼

㊽

㊾

㊿

1

2

3

4

5

6

7

8

9

10

11

12

13

14

15

16

17

18

19

20

21

22

23

24

25

26

27

28

29

30

31

32

33

34

35

36

37

38

39

40

41

42

43

44

45

46

47

48

49

50

51

52

53

54

55

56

57

58

59

60

61

62

63

64

65

66

67

68

69

70

71

72

73

74

75

76

77

78

79

80

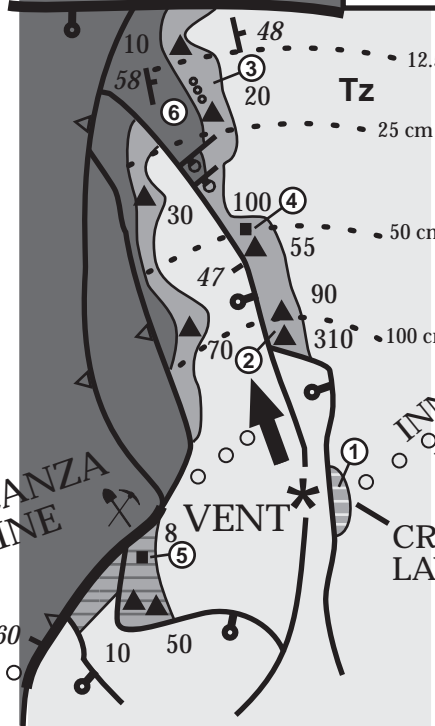
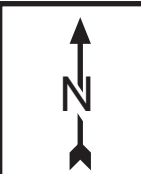
81

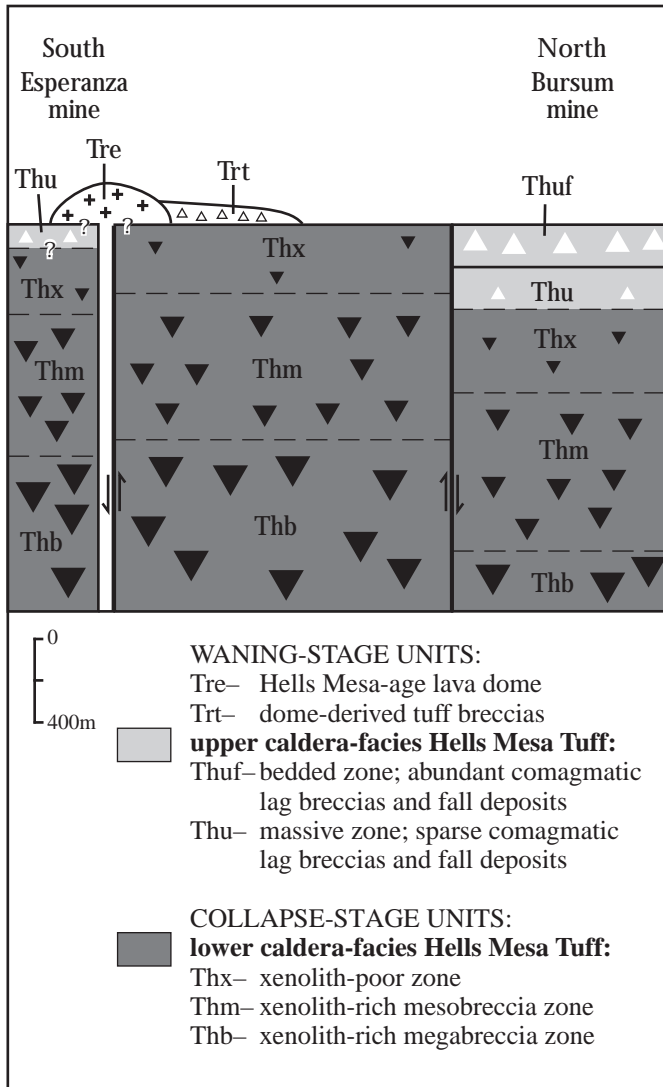
82

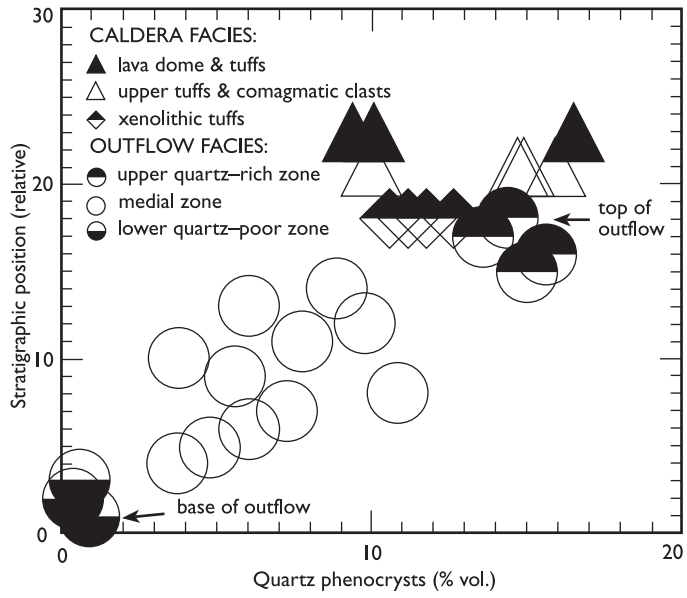
83

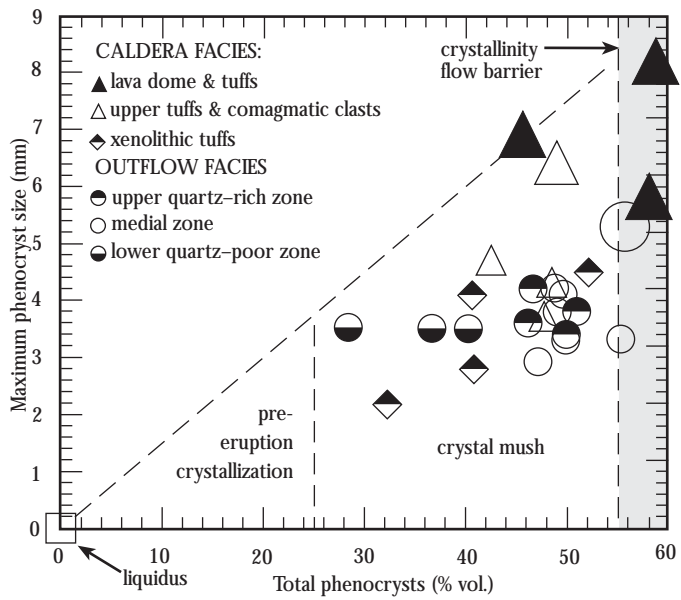
84

85

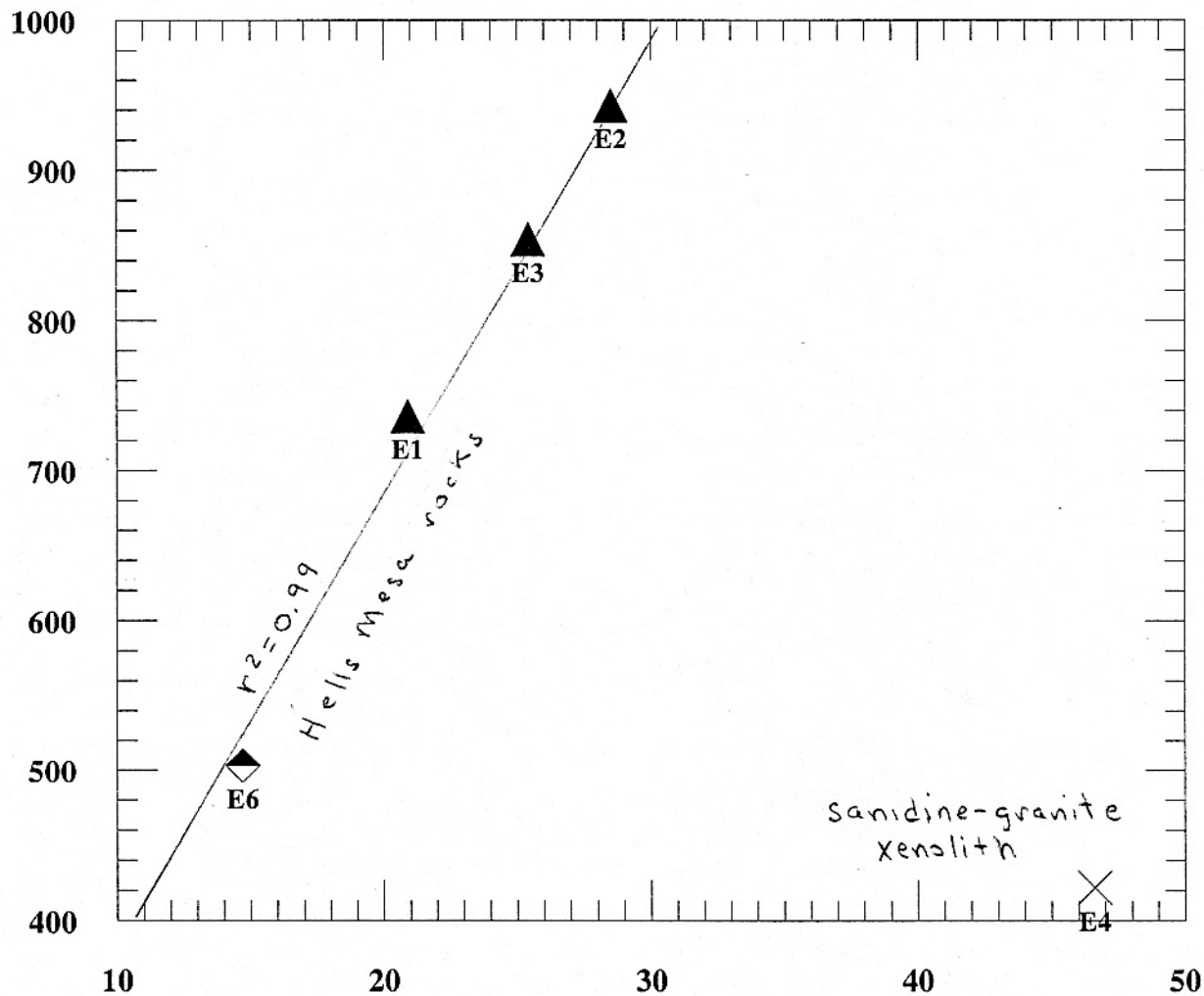






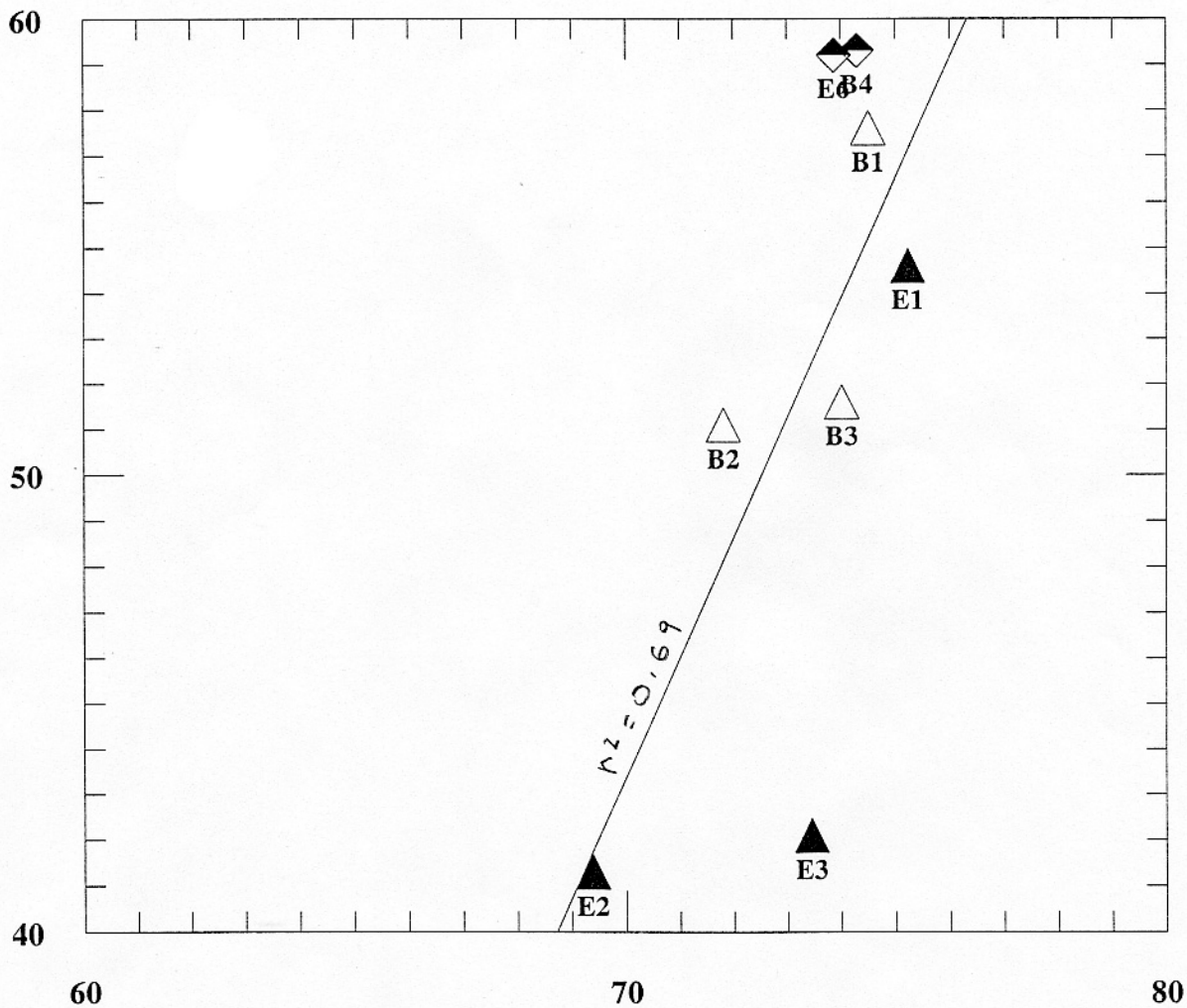


Ba (ppm)



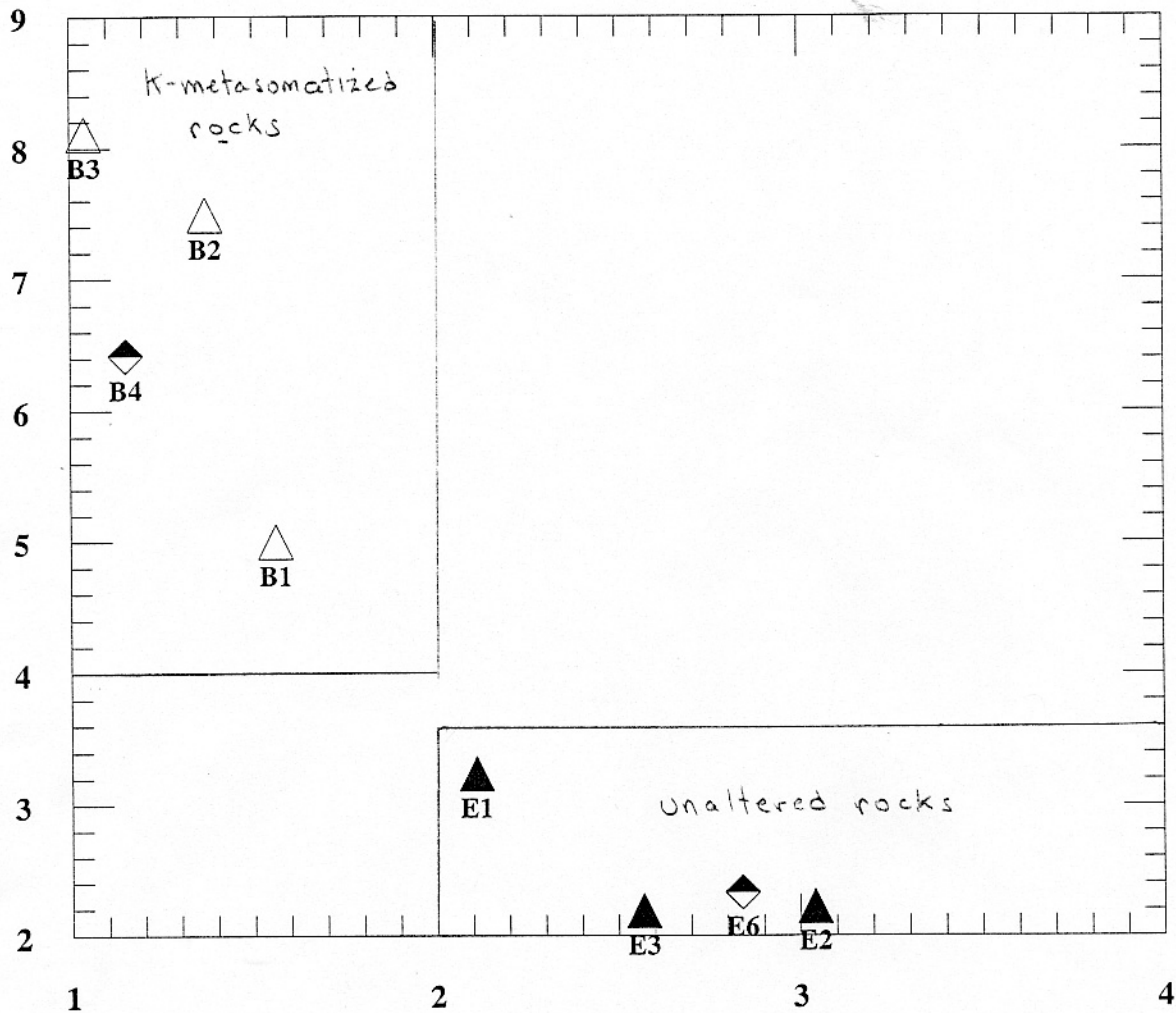
Sanidine (vol.%)

Groundmass (melt, vol. %)



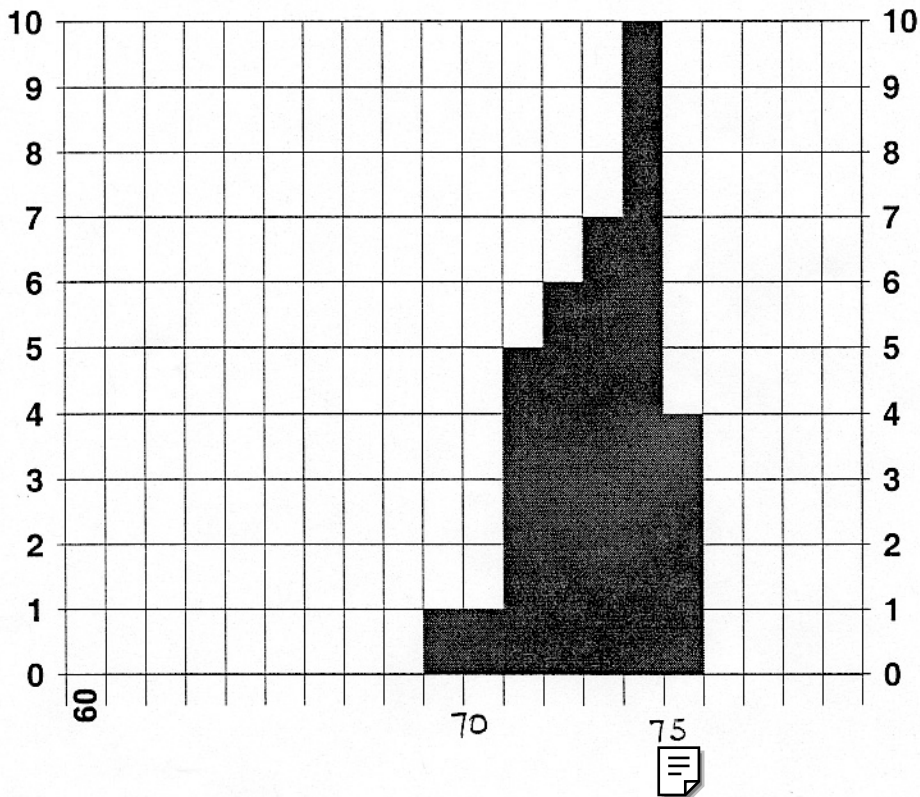
SiO2 (wt. %)

K₂O/Na₂O



Na₂O

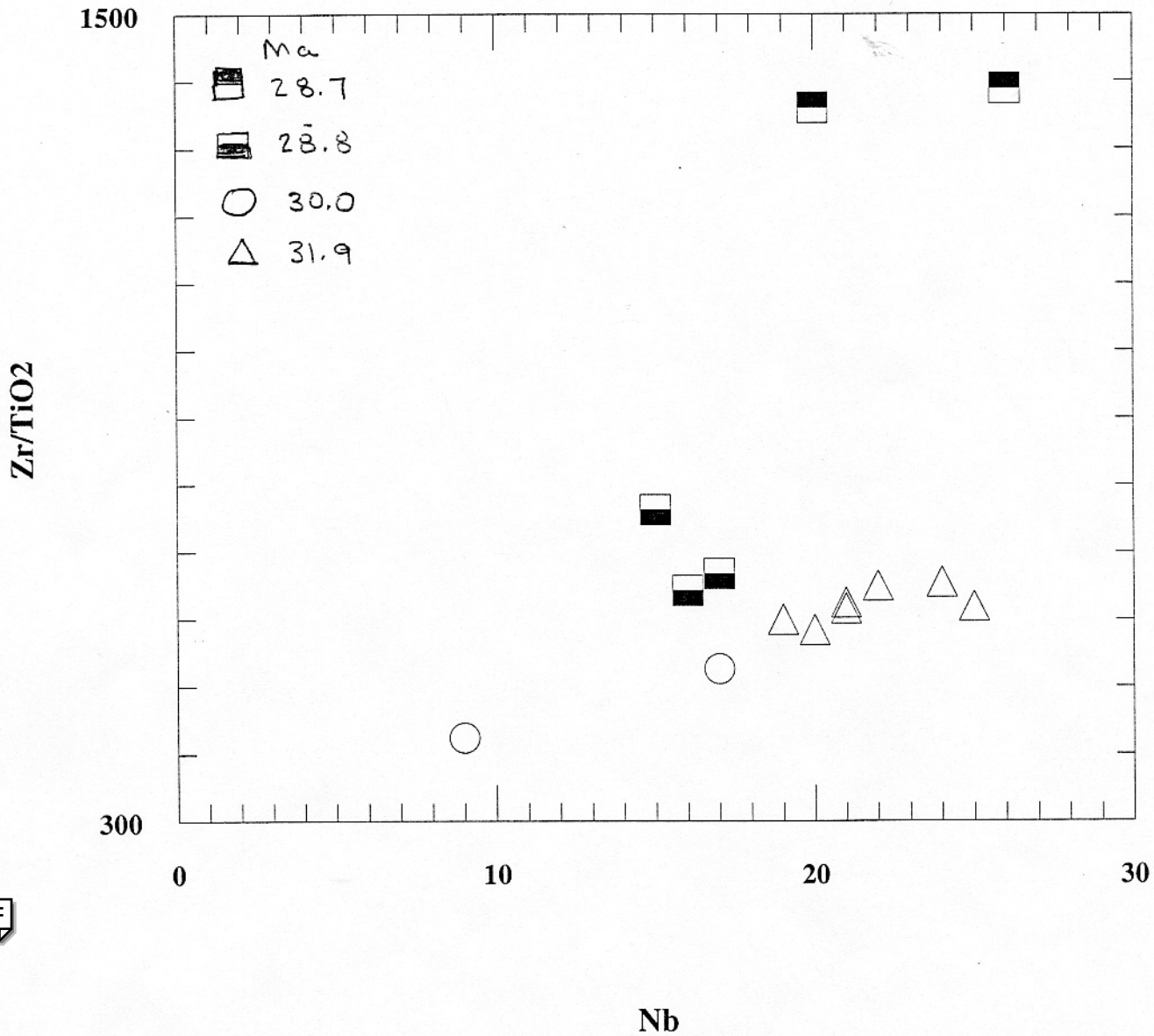
Hells Mesa magmatic suite (n=34)



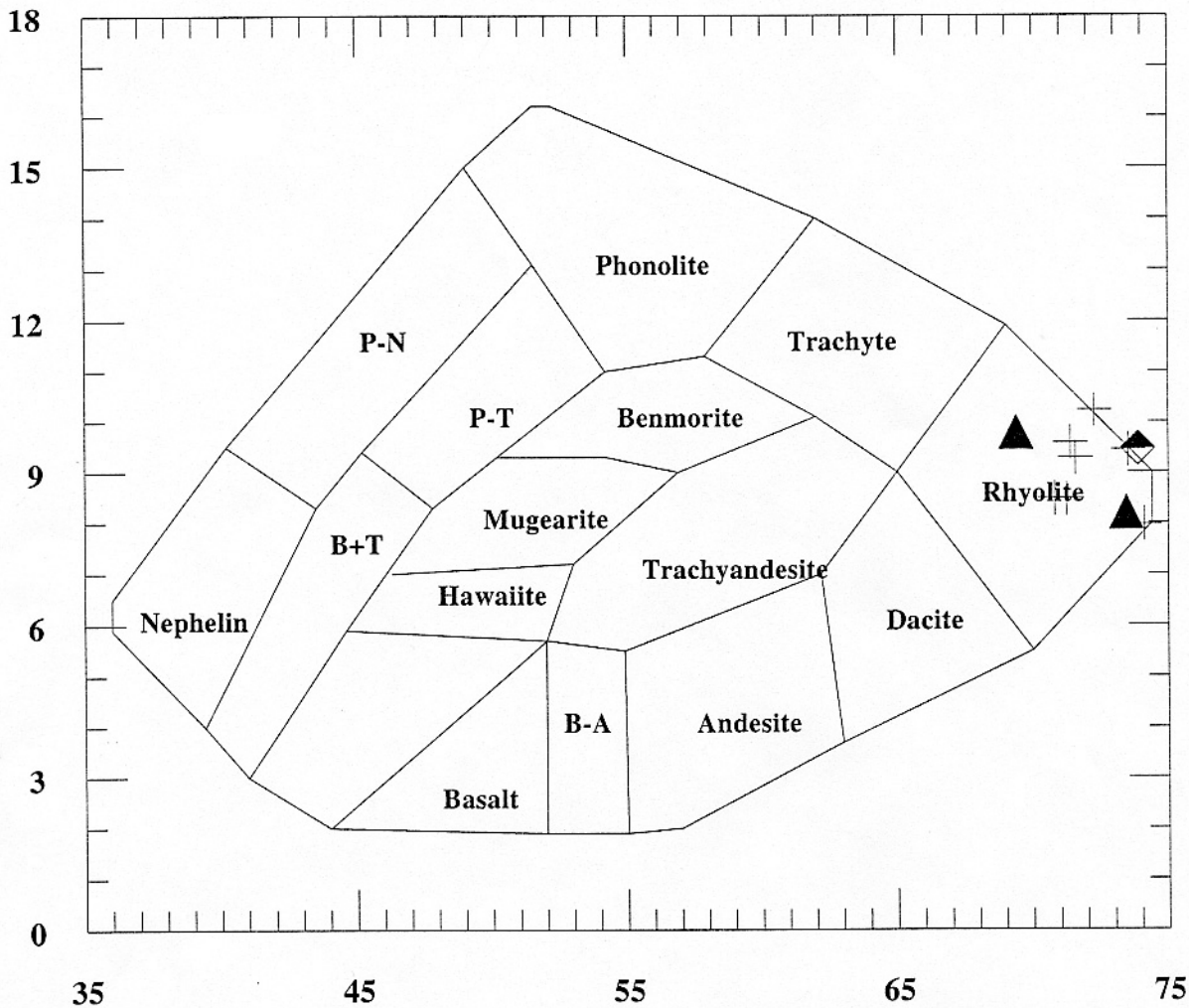
SiO₂ (wt %)

mean = 73.4 ± 1.5

normalized select data from Table 5



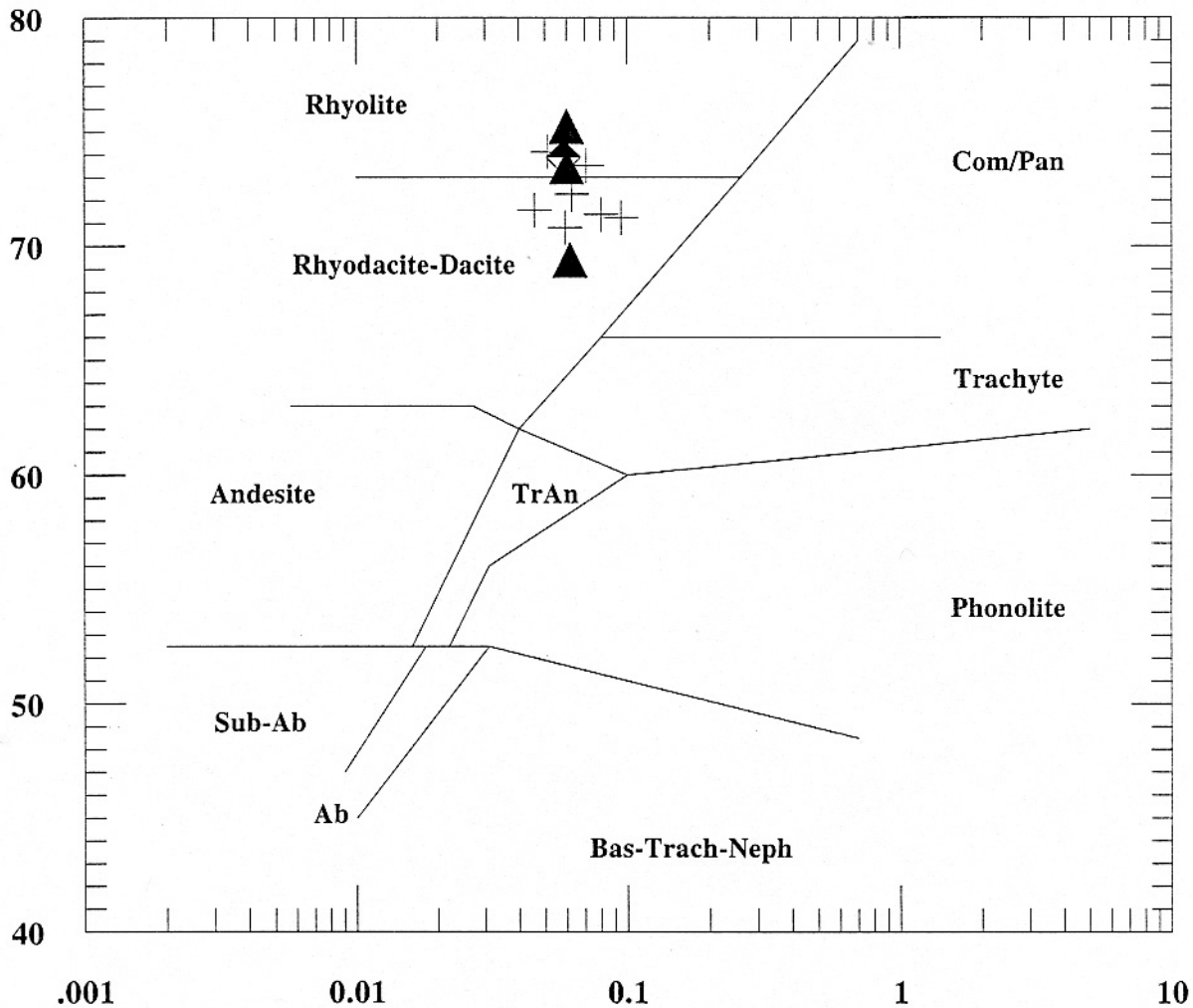
Na₂O+K₂O



SiO₂

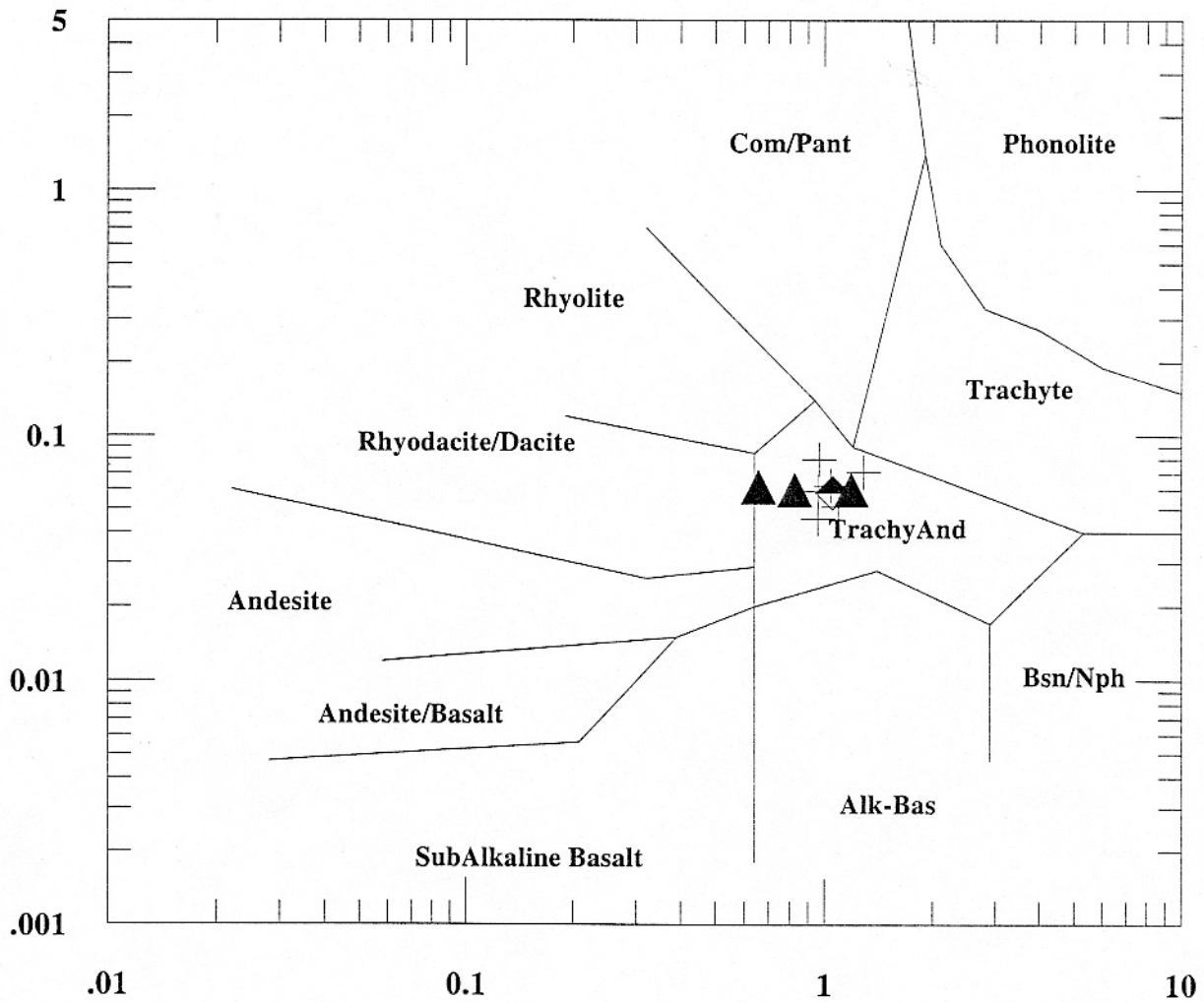


SiO₂



Zr/TiO₂*0.0001

Zr/TiO₂*0.0001



Nb/Y

